Research Article

P. Nimnate, T. Thitimakorn*, M. Choowong, and K. Hisada

Imaging and locating paleo-channels using geophysical data from meandering system of the Mun River, Khorat Plateau, Northeastern Thailand

https://doi.org/10.1515/geo-2017-0051
Received Apr 19, 2017; accepted Oct 24, 2017

Abstract: The Khorat Plateau from northeast Thailand, the upstream part of the Mun River flows through clastic sedimentary rocks. A massive amount of sand was transported. We aimed to understand the evolution of fluvial system and to discuss the advantages of two shallow geophysical methods for describing subsurface morphology of modern and paleo-channels. We applied Electrical Resistivity Tomography (ERT) and Ground Penetrating Radar (GPR) to characterize the lateral, vertical morphological and sedimentary structures of paleo-channels, floodplain and recent point bars. Both methods were interpreted together with on-sites boreholes to describe the physical properties of subsurface sediments. As a result, we concluded that four radar reflection patterns including reflection free, shingled, inclined and hummocky reflections were appropriated to apply as criteria to characterize lateral accretion, the meandering rivers with channel-filled sequence and floodplain were detected from ERT profiles. The changes in resistivity correspond well with differences in particle size and show relationship with ERT lithological classes. Clay, silt, sand, loam and bedrock were classified by the resistivity data. Geometry of paleo-channel embayment and lithological differences can be detected by ERT, whereas GPR provides detail subsurface facies for describing point bar sand deposit better than ERT.

Keywords: ERT, GPR, paleo-channel, meandered scar, floodplain

1 Introduction

Electrical Resistivity Tomography (ERT) and Ground Penetrating Radar (GPR) techniques have been widely used in the past for describing lithological and sedimentological characteristics of Quaternary deposits [3–5]. GPR detects changing of dielectric constant properties of sediment layers; therefore, the data will show discontinuities in the shallow subsurface. ERT is a particular useful survey method in clayey soil, where GPR is less effective. ERT technique commonly shows the variations of large scale sedimentary deposit [6]. These two geophysical methods are good combination for sedimentological investigations, particularly in place where variations in subsurface lithological conditions occur.

GPR signal responses can be directly related to change in relative porosity, material composition and moisture content [7], thus, it can also help to identify transitional boundaries in subsurface layers that can be difficult to detect by using other geophysical methods. However, geophysical survey interpreting in accordance with sedimentary data from boreholes is common and good combination to describe the fluvial geomorphology from subsurface. The geomorphology of paleo-channel is obviously distinct from floodplain area. The lower surface elevation and prominent boundary which is similar to river-shape is the primary feature of paleo-channel which can recognize from bird's-eye view.

Here in this paper, we aimed to understand the subsurface of sand-dominated fluvial system deposit along the Mun River on the Khorat Plateau. The advantage of two shallow geophysical methods (ERT and GPR) will be discussed. In this paper, paleo-channels, floodplains and recent point bars are of landform targets for both shallow geophysical investigations. ERT and GPR profiles will show the subsurface lithology, whereas sediment cores

***Corresponding Author: T. Thitimakorn:** Morphology of Earth Surface and Advanced Geohazards in Southeast Asia Research Unit (MESA RU), Department of Geology, Faculty of Science, Chulalongkorn University, Bangkok 10330, Thailand; Email: Thanop.t@chula.ac.th; Tel.: 66-02-218-5442; Fax: 66-02-2185464
P. Nimnate, M. Choowong: Morphology of Earth Surface and Advanced Geohazards in Southeast Asia Research Unit (MESA RU), Department of Geology, Faculty of Science, Chulalongkorn University, Bangkok 10330, Thailand
K. Hisada: Earth Evolution Sciences, Graduate School of Life and Environmental Sciences, University of Tsukuba, Ibaraki, Japan

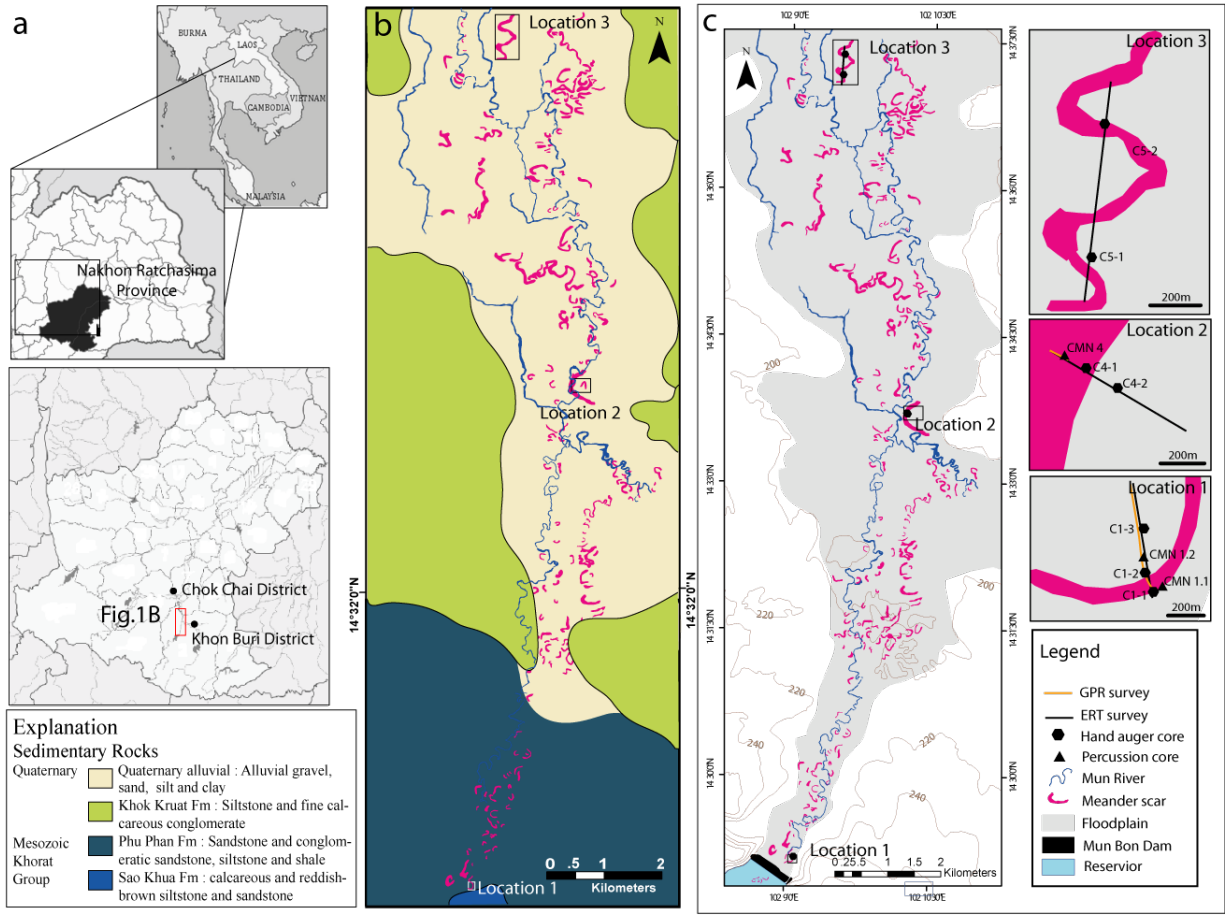

Figure 1: Location of the study sites in the Khon Buri District, Nakhon Ratchasima Province, Northeastern Thailand (a). Geology of the study area (b). Geomorphic map presents three locations of ERT, GPR survey and close up locations of sediment sampling (boreholes by hand auger and percussion cores) on the Mun River floodplain (c).

from boreholes are collected to compare and verify the geophysical interpretation. The upstream part of the Mun River was selected for this investigation because of less human activity affects. The shallow subsurface variation from geophysical survey will illustrate the profiles of fluvial deposition cross sections of pointbar, paleo-channel and floodplain. The depositional models were created from the relationship of electrical resistivity and sediment grain size. ERT lithological classes were identified by grain size analysis, and they expected to provide key for the resistivity model interpretation. The other purpose is to categorize GPR radar facies, and the sedimentary structures from point bar deposit especially from location 1.

The study area is located on Khorat Plateau which is the largest clastic sedimentary rock plateau in Southeast Asia. The plateau is elevated from a hundred meter above the present mean sea level. It is the main part of Indochina continent that was lastly uplifted by Himalayan orogeny. The plateau is mainly located in Thailand and partially extending to Laos PDR and Cambodia. In terms of geological structures, the plateau consists of two large synclinal basins. The southern basin has two main rivers; the Mun and the Chi. The Mun River is originated from the southwest rim cuesta of the Khorat Plateau. The Mun River scours into clastic rock basement providing a massive amount of sand transported via the river to form fluvial system on the low-lying plain downstream. Geomorphic feature such as various sizes of paleo-channels can be depicted from series of black and white aerial photographs (1974) on the recent floodplain [1].

The Mun River is the longest one flowing on the Khorat Plateau mostly in west to east direction. It is a tributary of the Mekong River [8]. The study area covers latitudes 14° 29' to 14° 37', and longitudes 102° 7' to 102° 10' (Figure 1). The southwest boundary of the study area starts from the Mun Bon Dam downstream to the north direction about 12

Figure 2: Photographs showings field investigation. (a) GPR survey using GSSI (SIR-20) instrument, (b) IRIS-SYSCAL R-1 Plus system of ERT survey, (c) line GPR and ERT survey from location 1, (d) ERT survey at location 2, (e) paleo-channel sediment from location 2 was drilled using hand auger, (f) longitudinal ERT line survey along the road at location 3, (g) sediment from three geomorphic units as point bar (C1-3 from location 1), paleo-channel (C4-2 from location 2) and floodplain (C5-1 from location).

km and 4 km wide of Khon Buri district. Rock basements are mainly composed on the Mesozoic Khorat Group (Phu Phan, and Khok Kruat formations) consisting of siltstone, sandstone, conglomeritic sandstone and shale [9]. These bedrocks are overlain by unconsolidated Quaternary alluvial sediment [10] (Figure 1(b)).

Paleo-channels (meandered scars) are the main target for shallow geophysical survey. From Figures 1(b) and (c), the distribution of paleo-channels was interpreted from aerial photographs taken in 1974 display mostly on the Mun river floodplain. Three shallow geophysics line surveys were selected (on the right side of Figure 1(c)). Location 1 is located near the Mun Bon Dam (Figure 2(c)). This survey line covers a paleo-channel and point bar. The other two areas are Ban Nong Sua Bong (Location 2) (Figures 2d and 2e) and Ban Wang Tabaek (Location 3) (Figure 2(f)) which are located in the northern side of the Mun Dam and on the right side of the Mun River floodplain. ERT and GPR line surveys from locations 2 and 3 cover the paleo-channels and floodplain. These locations 2 and 3 are

located far away about 200 m and 400 m from the Mun River, respectively.

2 Materials and methods

2.1 Electrical Resistivity Tomography (ERT)

ERT is a useful technique for providing information on the spatial and temporal variability of different zones: topsoil, active zone, bedrock, based on resistivity data and for reaching depths otherwise inaccessible[2]. In this study, three ERT profiles were obtained in three locations in the upstream area of the Mun River (Figure 1(c)). IRIS-SYSCAL R-1 Plus system (Figure 2(b)), metal electrodes, electric wires, hammer and direct battery were used. The purpose of ERT survey is to measure local resistivity exhibited by a material when an electric current passes through the sedimentary layer [11,12]. Electrode configuration was employed the dipole–dipole array, with an electrode spacing of l m, profile length of 94 m at locations 1 and 2, and electrode spacing of 2.5 m, profile length of 235 m at location 3. The dipole-dipole electrode array consists of two sets of electrodes, the current (source) and potential (receiver) electrodes. A dipole-dipole is a paired electrode set with the electrodes located relatively close to one another. The convention for a dipole-dipole electrode array is to maintain an equal distance for both the current and the potential electrodes (spacing = a), with the distance between the current and potential electrodes as an integer multiple of a. The advantages of the dipole-dipole electrode array are using shorter wire length if compared with other configurations and it is very sensitive to vertical change such as dike and cavity, thus paleo-channel body can be distinguished [13]. The current electrodes are used to introduce a current into the earth; while, the voltage or potential electrodes are used to measure the voltage which is calculated the local resistivity. ERT profiles have been interpreted based on the resistivity obtained during fieldwork and processed with RES2DINV computer software by using robust inversion method which obtain clear and linear border. The processing was based on absolute difference between measures and calculated apparent resistivity.

2.2 Ground Penetrating Radar (GPR)

GPR is a non-destructive method that analyses the underground propagation of high-frequency electromagnetic wave in the frequency range of 100 MHz to 2 GHz. The device is equipped with an emitting antenna that moves across the surface of the terrain and emitted very short temporal pulses. The contrasting in the dielectric constant usually causes reflections from lithological boundaries in the subsurface [14]. The reflection records by a receiver antenna. Depth of GPR is dependent on the antenna frequency [15]. A higher frequency of the antennas resulted in a higher resolution, but the penetration depth decreased. In contrast, the low frequency decreases the resolution, and the survey depth is deeper [16]. GPR has been used to analyze fluvial facies [15, 17–23]. However, silt and clay depositions cause attenuation of the radar signal which limits the depth range of measurement but can also be useful to determine the thickness of alluvial fill [24]. As for the bulk dielectric constant of common earth materials for GPR that measured at 100 MHz of dry soils (sandy, loamy and clayey) is approximately 4 to 6. On the other hand for the wet soil, the dielectric constant of sandy, loamy and clayey wet soils are 15-30, 10-20 and 10-15, respectively [25]. However, for time to depth conversion, the dielectric constant of the subsurface has to be determined. In this study, the dielectric constant was determined based on drilled cores along the GPR survey lines. As a result, the average dielectric constant used in this study was 8.

In this study area, two GPR profiles were measured at point bar and paleo-channel from location 1 and paleo-channel in Ban Nong Sua Bong from location 2 (see Figure 1(c) for location). Profile lengths were set at 120 m and 15 m, respectively, and surveyed on the ground level approximately 30 cm higher than the normal rice filed. Sets of profile were obtained by using a GSSI radar system with a 200 MHz antenna (Figure 2(a)). GPR field data were processed by using the RADAN program of the Geophysical Survey System Inc. All data require processing in order to sharpen the signal waveform by improving the signal to noise ratio [26]. The raw data were filtered using such as background removal, band pass filter, migration, hyperbolae removal and range grain before interpretation. Sedimentary successions from boreholes were used to interpret with GPR and ERT profile.

GPR profiles were interpreted and categorized the radar reflection patterns. The various radar reflection types of fluvial deposit structures are recognized as “radar facies”. The continuity shape, amplitude and configuration of internal reflection used to distinguish the radar facies [14, 18, 27]. Radar facies interpretation is based on the principles of radar stratigraphy [18, 28] The radar facies were compared with charts relating the reflection configuration on the radar record from the previous works [29, 30]. GPR data had high vertical and horizontal resolution (on the order of decimeters). Conversely, resistivity data pos-

sess relatively low vertical and horizontal resolution (on the order of meters) but they are sensitive to lithological information such as relative clay percentage. GPR data also image stratigraphic variation to a higher degree, while ERT data collected here tends to blur those boundaries [31]. The integration of the two geophysical datasets together with the drilling information allows a comprehensive sedimentological and lithological characterization of the subsurface.

2.3 Stratigraphy and sediment description

Sediment sampling was carried out with a hand auger and percussion drilling, directly below the respective ERT profiles on each geomorphic unit (Figure 2(g) [2]). Nine boreholes were drilled from 3 locations. ERT and GPR lines are assigned as close as possible to borehole locations. A total 51 sediment samples were analyzed by Particle size distribution by laser diffraction. This laser diffraction technique is based on the principle that particles passing through a laser beam will scatter light at an angle that is directly related to the sediment size. The sediments are mostly prepared with water as suspensions, and a small ultrasonic treatment is sometimes useful in breaking up loosely-held agglomerates. A few millilitres of suspension are required to carry out the measurements. After that these samples were subsequently classified under the Shepard's classification system for sand, silt and clay for distinguishing the sedimentary type [3, 32, 33]. The lithological logs from boreholes were used to verify the lithologic types and boundary of GPR and ERT profiles. These lithological logs were scaled and superimposed on GPR and ERT profiles.

3 Results

3.1 Raw data initial interpretation

3.1.1 Stratigraphy and physical properties of sediments

Characterizations of nine boreholes are based on laser particle size analyzer from 51 samples, and the proportions of sand silt and clay were classified under the Shepard's classification system modified by (Figure 3). Boreholes C1-1, CMN1, C1-2 and C1-3 are located on location 1 (Near Mun Bon Dam). Boreholes CMN4, C4-1 and C4-2 are drilled on location 2 (Ban Nong Sua Bong). Boreholes C5-1 and C5-2 are gathered from location 3 (Ban Wang Tabaek).

Sediment cores from location 1 were drilled on the paleo-channel (CMN1) and point bar (C1-1, C1-2 and C1-3) (Figures 6a and 7a). In general, on point bar deposit as C1-1 and C1-2 boreholes are dominated by silty sand, loam, clayey sand, and sand, while C1-3 core is dominated by loam, this term represents the mixture of sediment consisting of sand, clay, and decaying organic material, in the upper part. The lower part is composed of sandy clay, silty sand and clayey silt. However, CMN1 is composed of sandy to silty clay and silty sand from paleo-channel location.

From sedimentological data from location 2 (Figure 6(b)), three boreholes were drilled from paleo-channel. CMN4 was collected the sediment from rice field. It is composed of sandy clay and clayey sand. CMN4, C4-1 and C4-2 are dominated by loam and clayey sand with some iron concretion-baring in loam layer from the 1.4 to 2.3-meter depth.

Two boreholes were gathered from floodplain (C5-1) and paleo-channel (C5-2) at location 3 (Figure 6(c)). Based on the sedimentary log from floodplain location, the finer sediment that is dominated by clayey silt with loam and silty clay in C5-1. On the other hand, C5-2 is mainly composed of coarser sediment as sand (clayey to silty sand) and silt (clayey to sandy silt) and loam from the paleo-channel location.

3.1.2 ERT profiles

ERT profiles were gathering during field with dipole-dipole array by IRIS-SYSCAL R-1 Plus system. Detail geophysics description from raw data of three ERT profiles is explained as follows.

Location 1: Near the Mun Bon Dam

Profile Line −94 m surveys across the paleo-channel and point bar in almost NS direction (see Figure 1 for location and Figure 2(c) for field area). Result of resistivity can be separated into three zones as top, middle and bottom from the ERT data in figure 4(a) and it shows low to high resistivity. At the top zone of ERT profile from 3 to −3 m presents moderate to high resistivity about 100-1200 Ω·m (in central to western sides). Then it changed the resistivity value to low resistivity (0-26 Ω·m) in the western side continued to middle to bottom of ERT profile presenting moderate to low resistivity (0-93 Ω·m) from −3m to −15 m. The bottom (left and right) of profile shows high resistivity approximately 120-1200 Ω·m.

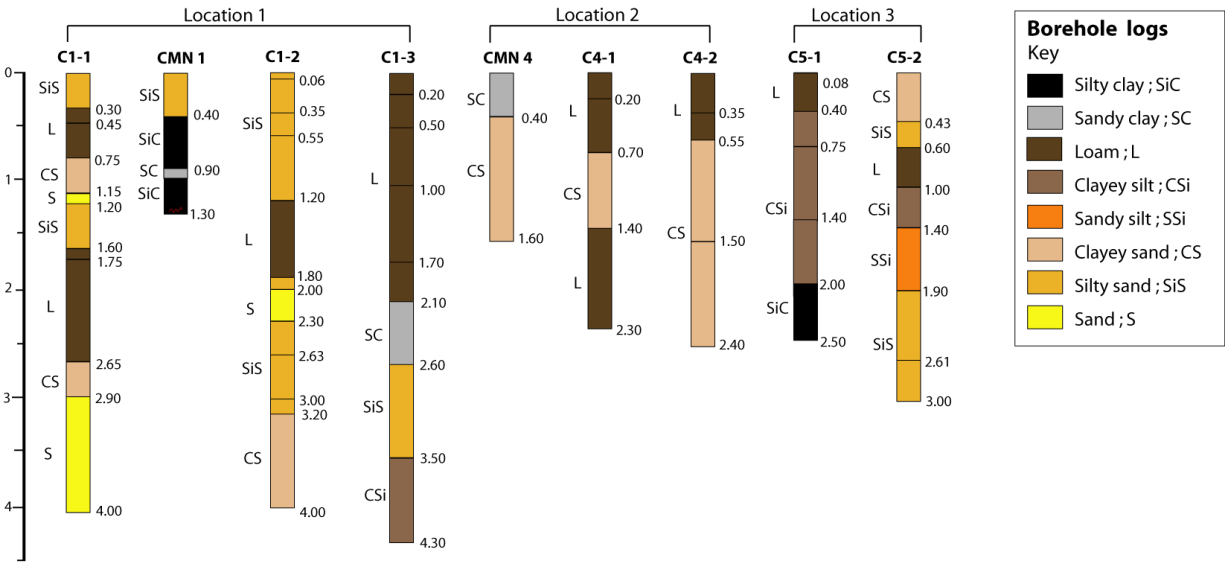

Samples classified under the Shepard's Classification System modified by Flemming (2000) :

C1-1 : SiS-Silty sand; L-Loam; CS-Clayey sand; S-Sand; SiS-silty sand; L-Loam; CS-Cleyey sand; S-Sand
CMN 1: SiS-Silty sand; SiC-Silty clay; SC-Sandy clay; SiC-Silty clay
C1-2 : SiS-Silty sand; L-Loam; SiS-Silty sand; S-Sand; SiS-Silty sand; CS-Clayey sand
C1-3 : L-Loam; SC-Sandy clay; Sil-Silty-sand; CS-Clayey sand
CMN 4 : SC-Sandy clay; CS-Clayey sand
C4-1: L-Loam; CS-Clayey sand; L-Loam
C4-2 : L-Loam; CS-Clayey sand
C5-1 : L-Loam; CSi-Clayey silt; SiC-Silty clay
C5-2 : CS-Clayey sand; SiS-Silty sand; L-Loam; SSi- Sandy silt; SiS-Silty sand

Figure 3: Boreholes drilled in the three locations; Near the Mun Bon Dam (location 1: C1-1, CMN1, C1-2 and C1-3), Ban Nong Sua Bong (Location 2: CMN4, C4-1 and C4-2) and Ban Wang Tabaek (Location 3: C5-1 and C5-2). These cores were drilled along GPR and ERT lines. Sediment classes are generalized from laser particle size distribution analysis using the Shepard's classification by Flemming [33]. The color scheme presented was also used for the interpretation of ERT data.

Location 2: Ban Nong Sue Bong

This survey line runs in nearly northwest - southeast direction across paleo-channel (Figure 1(c)). ERT profile at Ban Nong Sue Bong is 94 m in length (Figure 2(d)). Medium to high resistivity zone (50-180 Ω·m) was drilled within clayey sand and Fe concretion bearing loam layers from boreholes C4-1 and C4-2 near GPR and ERT line survey. This zone was surrounded by lower resistivity zone which is dominated by the value of resistivity less than 36 Ω·m. The bottom left and right of ERT profile show high resistivity value (>120 Ω·m) occurring at 10-20 m from a surface.

Location 3: Ban Wang Tabaek

ERT line runs 235m along floodplain. Survey line was made in longitudinal profile of paleo-channel in the north-south direction (Figure 2(f)). Result of ERT profile (Figure 6(c)) shows high resistivity value from 100-160 Ω·m at near the surface to 10-meter depth. The lower resistivity shows value from 30-50 Ω·m.

3.1.3 GPR profiles

Location 1: Near the Mun Bon Dam

GPR profiles were surveyed on point bar and paleo-channel. Locations and direction of GPR profiles are illustrated in Figures 1a and c. GPR result from location 1 surveyed on the paleo- channel and point bar almost NS direction 120 m (Figure 5(a)) shows a maximum depth of 4.40 m. Three different zones can be distinguished depending on the contrast of GPR signal. Uppermost zone of GPR profile presents obscure radar reflection, so the faded parallel can be observed from the upper part. This zone is affected by earth-filled for agriculture. Low angle dipping reflection (10° to 45°) from surface of silty sand and loam layers show inclination and discontinuous reflection pattern between 1.5 to 2.5 m in the middle zone (no. 2, 3 and 4). Sediment layer dips eastward into the paleo-channel. The lower zone of profile displays poor reflectivity because sediment layer cannot be observed from water saturated silt and sand from 2.5 to the deeper area (no. 1).

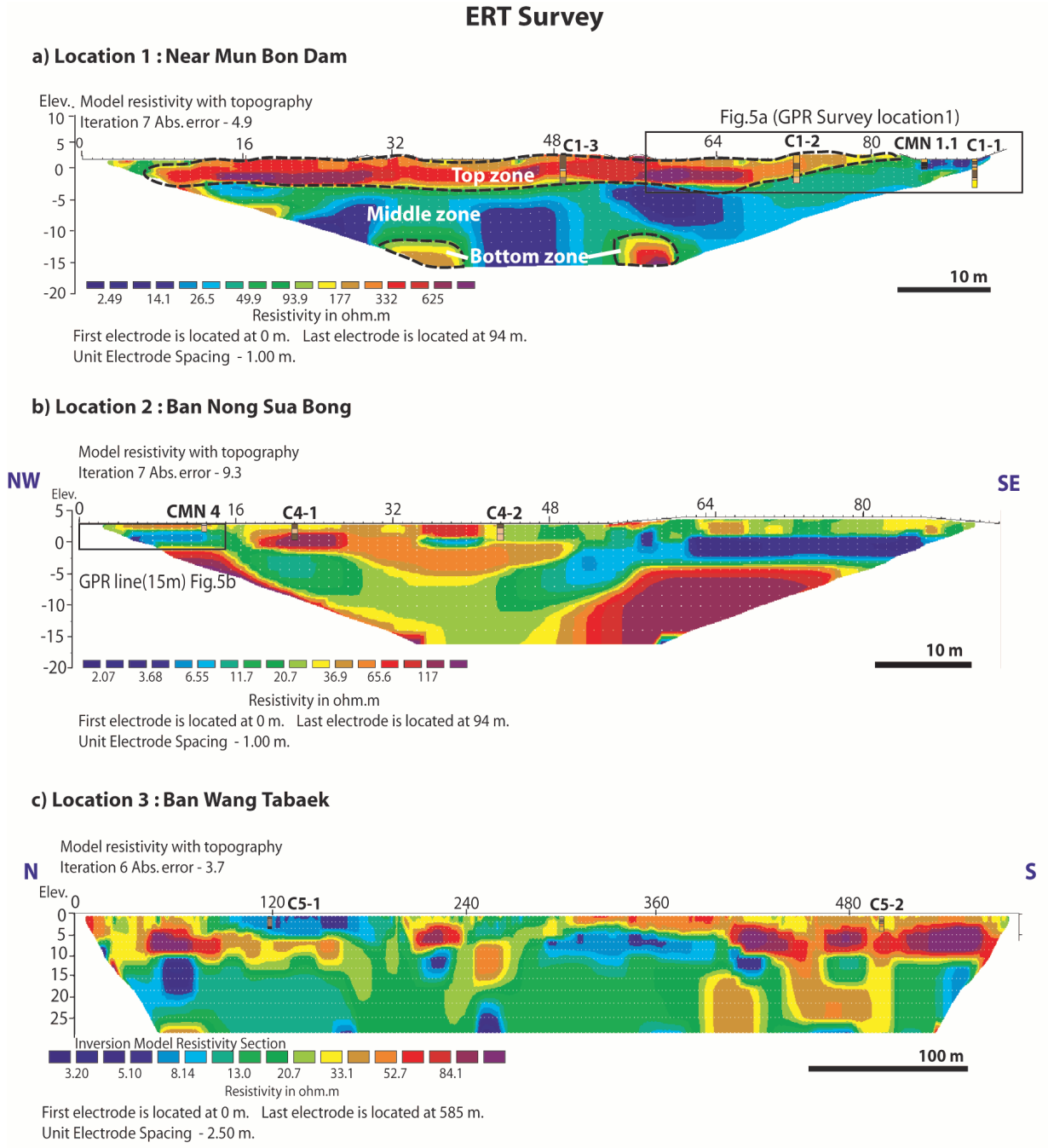

Figure 4: ERT profiles from three location a) near Mun Bon Dam, 94m-ERT surveyed on paleo- channel and point bar, b) Ban Nong Sue Bong where paleo-channel was investigated (94 m) and c) Ban Wang Tabaek, 585m-ERT profile survey over floodplain and paleo-channel (longtitudinal profile).

Location 2: Ban Nong Sue Bong

This GPR profile was gathered on paleo-channel in the NW/SE direction (15 m long). Figure 5b displays parallel and unclear reflections in the upper zone, and this radar signal came from the surface of earth-filled which has high lateral variation of dielectric constants. Sediments were classified as loam layer. The middle zone from 2 to 3 m was illustrated as thick black and white quite parallel orientation and, it shows slightly wavy reflection in some parts corresponds to sandy clay and clayey sand from CMN4. These two layers were overlain on the poor reflection of water saturated clayey silt from 3m depth.

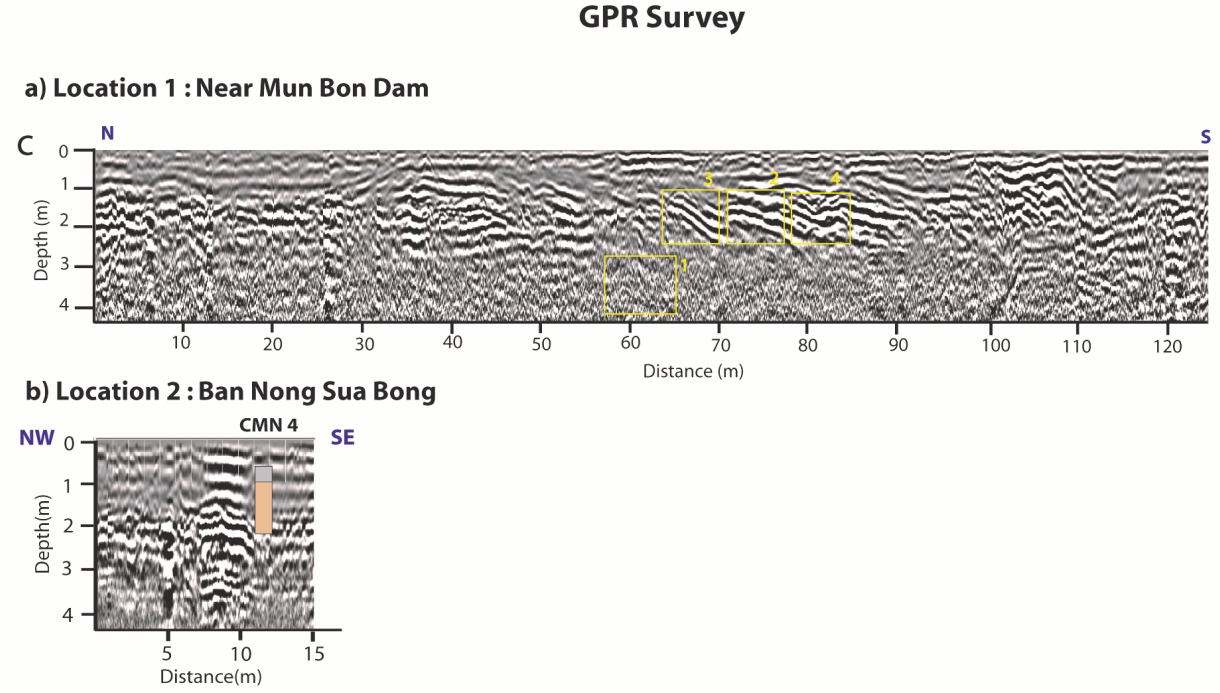

Figure 5: Two GPR profiles collected from locations 1 and 2. Point bar and paleo-channel at Ban Nong Sue Bong show 125 m and 15 m GPR long profiles collected with 200 MHz antenna.

3.2 Modelling description and outcomes

Depositional models were interpreted based on sediment grain size and electrical resistivity values. The color scheme in Figures 3, 5, 6 and 7 represents lithological data of ERT inversion models gathering from boreholes. Detail geophysics description from three ERT profiles is explained as follows.

Location 1: Near the Mun Bon Dam

Cross-section model displayed the sedimentary deposit across the paleo-channel and point bar in almost NS direction (Figure 6(a)). Result of resistivity and sediment grain-size can be separated into three zones as top, middle and bottom. Moderate to high resistivity of top layer from 3 to −3 m associated with loam and silty sand of topsoil layer. The resistivity value in the western side relates to silty clay of channel filled deposit from the borehole CMN1 (Figure 4(b)). The middle to bottom of model presents clayey silt, clayey sand and silty sand of point bar deposit. At the bottom (left and right) of profile shows high resistivity which interpreted as sandstone bedrock.

Location 2: Ban Nong Sue Bong

Model of paleo-channel and floodplain at Ban Nong Sua Bong is 94 m in length (Figure 6(b)). Clayey sand and Fe concretion bearing loam layers from boreholes C4-1 and C4-2 near associated with paleo-channel in Figure 6b. Width and depth of paleo-channel are approximately 30 m long and the depth ranges between 0-10 m. This zone was surrounded by lower resistivity zone of floodplain deposit which is silty clay and clayey silt. The bottom left and right show high resistivity and it was interpreted as sandstone bedrock.

Location 3: Ban Wang Tabaek

Fluvial depositional model of paleo-channel floodplain displays the longitudinal profile in the north-south direction (Figure 6(c)). High resistivity value associated with loam and clayey to silty sand layers, and it was interpreted as paleo-channel. Approximate depth of channel appears from 5 to 10 m. Moreover, the deeper channels were found at 20 to 25 m from the surface. On the other hand, the fined grain sediments such as silty clay, sandy clay and clayey silt from C5-1 surrounded paleo-channel belong to floodplain deposit.

3.3 GPR profiles interpretation

Location 1: Near the Mun Bon Dam

On point bar and paleo-channel, three sediment layers are distinguished from GPR result (Figure 7(a)). Uppermost zone of GPR profile presents is disturbed by top soil

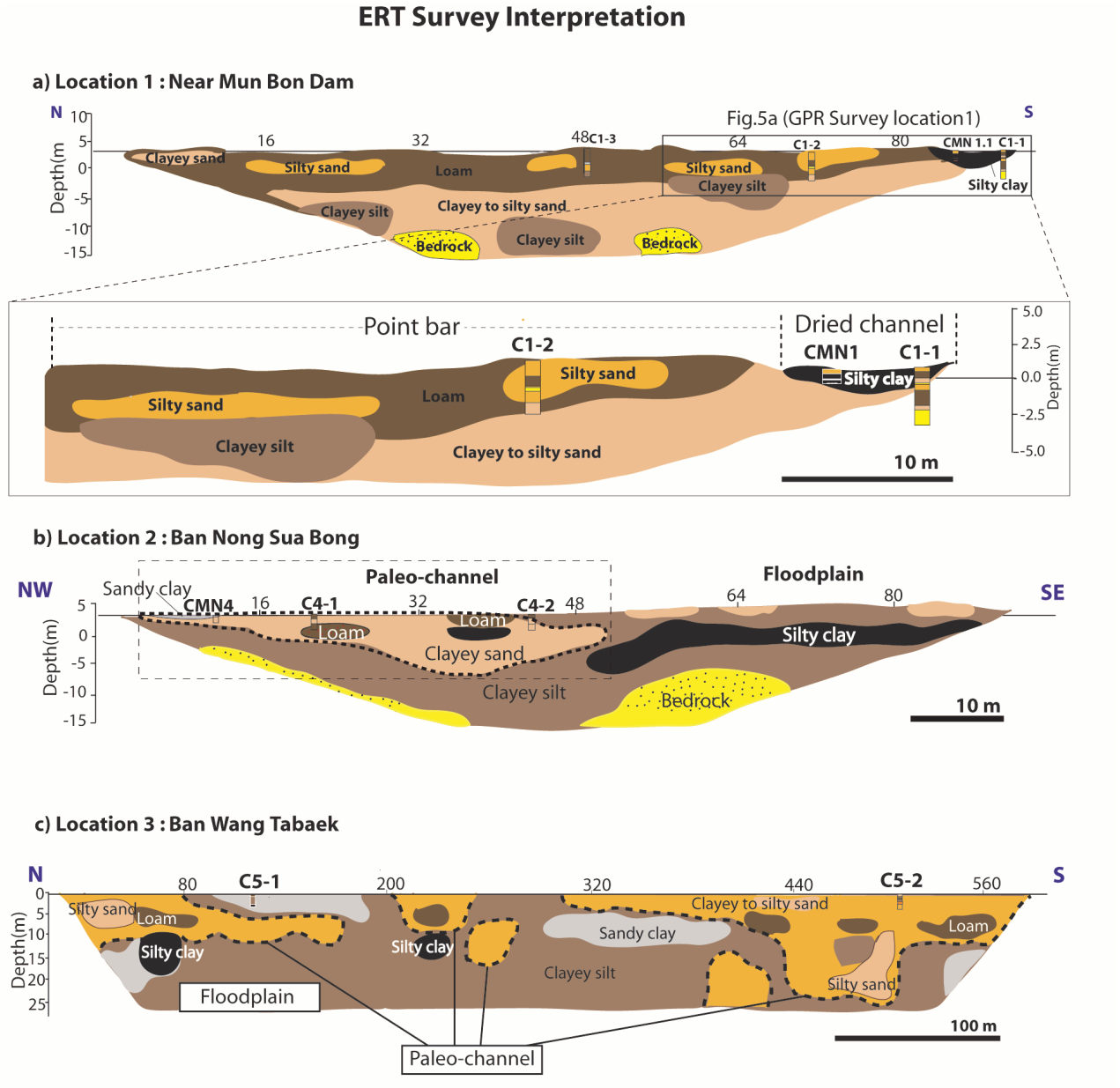

Figure 6: Interpreted three ERT profiles as cross-section from point bar, paleo-channel and floodplain modelling based on resisitivity valued and boreholes data. a) 94 m long profiles near Mun Bon Dam. (b) 94 m long profiles at Ban Nong Sue Bong. c) 585 m profiles interpretation at Ban Wand Tabeak.

from agriculture. In the middle zone, Low angle dipping reflection and discontinuous reflection pattern between 1.5 to 2.5 m were interpreted as lateral accretion of point bar deposit. The lower zone is water saturated zone.

Location 2: Ban Nong Sue Bong

This GPR profile was gathered on the rim of paleo-channel. The radar displays parallel and unclear reflections in the upper zone. At the abscissa of about 10 m, the radar signal shows an inversion of polarity of the electromagnetic wave. Because of this radar signal came from very near surface top soil which has high lateral variation of dielectric constants and also it is the cause of an inversion of GPR signal. The middle and the bottom zone which consists of sandy clay and clayey sand were interpreted as floodplain deposit (Figure 7(b)).

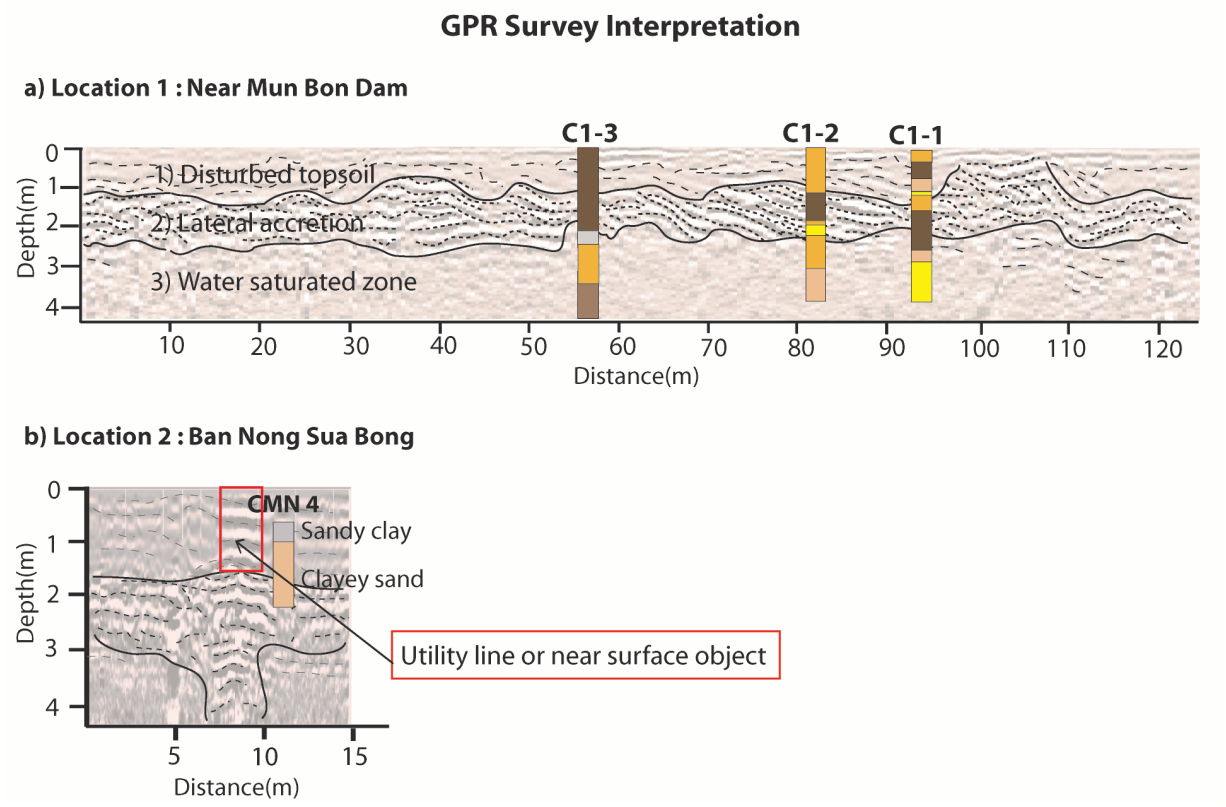

Figure 7: GPR interpretation model from 2 locations. Three layers of point bar deposit were classified from Mun Bon Dam area. At Ban Nong Sue Bong was surveyed on paleo-channel covered by high clay content sediment.

Table 1: ERT lithology classes and GPR redar facies identified in the study area.

Resistivity (Ωm)	ETR lithological classes
0-11	Clay (Silty to Sandy clay)
11-33	Silt (Clayey silt to Sandy silt)
20-120	Sand (Clayey sand, Silty sand and Sand)
62-160	Loam
120-160	Bedrock

4 Discussions

4.1 Relationship between fluvial sediment and ERT lithological classes

We attempted to relate sediment properties of subsurface fluvial sediment from nine boreholes and results of ERT surveys are shown in Table 1 and Figure 6. ERT profiles show thickness of fluvial deposit from 5 to 30 m depth and clearly reveal vertical and horizontal changes. However, the detail of sedimentary internal structure cannot be recognised using this technique alone [3]; however, the GPR can be the supplement. Based on resistivity profile results from location 1 (Figure 4(a)), the upper most part, the cultivated soil with low moisture contents depicts high resistivity value (orange to purple color). This zone was interpreted as point bar deposit and it is concordant with GPR and sedimentological data from boreholes. Point bar sediments consist mainly of sand (clayey to silty sand) and loam in C1-2 and C1-3. The middle zone of ERT profile in location 1 displays low resistivity (blue to green color) because the pores between sediment grains are saturated with groundwater, therefore, the higher resistivity shows in this zone Composition of sediments is associated with higher clay content such as clayey silt and clayey to silty sand than the upper part. High resistivity value (orange to purple color) from the bottom part of profile was related to bedrock which is mainly composed of sandstone, siltstone and conglomeritic sandstone of Phu Phan formation [34].

Based on ERT surveyed across paleo-channel at location 2 (Ban Nong Sue Bong), the outcome displays medium to high resistivity value body. It shows channel-liked shape of buried paleo-channel from the surface to 10 m depth in yellow to dark red color (Figure 4(b)). Sediment mainly

GROUP	SCHEMATIC EXAMPLE	GPR FACIES	DESCRIPTION	INTERPRETATION (Bere and Heani, 1991; Hickin et al., 2009)
Reflection free	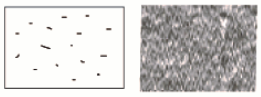	Facies 1 Reflection free	High conductive loses Poorly defined reflection pattern and lack of penetration profile	1. Attenuated energy 2. Massive homogeneous l lithological unit 3. High clay content
Layer reflection				
Clinoform	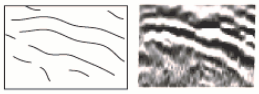	Facies 2 Shingled reflection	Short (5-10m) incline (5-20 degree) shingled reflections	- Well to moderate stratified stratified dipping bedding, lateral accretion, slipface of migration bedform
	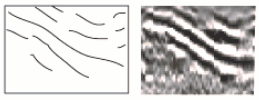	Facies 3 Incline reflection	Short (<10m) sigmoid oblique, tangential or parallel, incline (15-45 degree) reflections	- Well to moderate stratified dipping, lateral accretion slipface of migration - Migration of channel bar, modern floodplain
Discontinuous	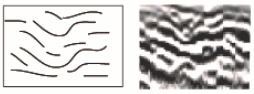	Facies 4 Hummocky reflection	Discontinuous (5-20 m), hummocky or disrupted relfections	- Sand bed or gravel bed - Crudely stratified to massive deposit obscured by diffractions

Figure 8: Three groups of radar facies and their interpretation from GPR reflection patterns of point bar deposit in the study area. Radar facies is classified based on Milan Beres and Heani and Hickin *et al.* [18, 29].

consist of clayey sand and loam layers deposited in channel (C4-1 and C4-2). This paleo-channel was enclosed with low resistivity value displays in green to blue color. Finer grain sediment as clayey silt and silty clay can be carried during flood and suspended in the moving water which rises above the channel and being to spread out. Finally, this fine grain sediments deposit along the parallel channel and form floodplain [35]. The bottom part of profile also displays high resistivity of pebbly sandstone bedrock consisting of siltstone and sandstone [34].

The longitudinal ERT profile of location 3 was carried out in floodplain of the recent Mun River at Ban Wang Tabaek (Figure 4(c)). High to moderate resistivity value (yellow to purple color) was interpreted as in-channel sediment deposition which is composed of loam and clayey to silty sand (Figure 6(c) (C5-2)). On the contrary, low resistivity value (green to blue color in Figure 4(c)) is associated with fine grain deposit such as clayey silt and silty clay (Figure (6) (C5-1)). Floodplain sediment is associated with loam, clayey silt and silty clay deposited on both sides of floodplain in C5-1. On the other hand, paleo-channels deposit comprises coarser sediments such as loam, sand (clayey to silty sand) and silt (clayey to sandy silt) in C5-2.

The integration of stratigraphy and sediment properties defined from nine boreholes, and three resistivity profiles of ERT survey allow us to distinguish ERT lithological classes of subsurface sediments in the study area. Resistivity values for the lithological types are defined in Table 1. Five lithological classes were deduced from the relationship between sediment grain size and their electrical resistivity properties. Clay, silt, sand, loam and bedrock demonstrated the results of resistivity ranges were demonstrated as 0-11 Ω·m, 11-33 Ω·m, 20-120 Ω·m, 62-160 Ω·m, and 120-160 Ω·m, respectively.

4.2 GPR radar facies of fluvial deposit

Based on radar reflection patterns, radar facies were mainly interpreted from location 1. Radar facies from fluvial deposit can be divided into three groups (reflection free, layer reflection and discontinuous) (Figure 8). Firstly, reflection free (Facies 1) represents the zone of attenuated energy from sediments contain high clay content or highly conductive dissolve mineral in groundwater (water saturated zone). Secondly, layer reflection shows inclination of radar pattern, and it's called a clinoform. The clinoform can be separated into two facies (shingled and incline reflections) which depends on dip angle of sediment layer. Shingled reflection (Facies 2) displays the inclination angle approximately 5-20 degree. Inclined reflection (Facies 3) exhibits sigmoidal oblique or parallel layer with dipping angle approximately 15-45 degree. These two clinoform reflections were interpreted as well to moderate stratified dipping bed which is formed by lateral migration process on point bars. Finally, hummocky reflection (Facies 4) of

discontinuous group shows discontinuous or disrupted reflections. This radar facie was interpreted as crudely stratified sand or gravel bed deposit with obscured by diffraction. GPR reflection patterns on the radar record of point bar deposit (Figure 7(a)).

At location1 (Figure 7(a)), the upper most part of radar pattern appears parallel layer of disturbed soil from human activity. The middle zone shows more clearly radar signal than upper and lower zones. The middle layer displays the dipping layer from loam and silty sand layers. It consists of three radar facies as shingled, incline and hummocky reflections from 1 to 2.5 m. A set of discontinuous to moderate continuous reflectors dipping 20 to 45 degrees in the east direction to the paleo-channel were depicted on the central part of the GPR profile. Shingled, incline and hummocky reflections occur in the loam dominated layer. Parallel and clinoform reflections (radar facies 2 and 3) were interpreted as well to moderate stratified dipping of lateral accretion of point bar. Hummocky (radar facies 4) was interpreted as sand or gravel bed.

Reflection free (radar facies 1) appears in the bottom zone. It results from attenuated energy from higher clay content (clayey to sandy silt). Shallow water Table makes the difficulty to pick out radar recorded in this location. For example, location 2 (Ban Nong Sua Bong), GPR line was surveyed on the rice including fine-grained (sandy clay filled over clayey sand in paleo-channel (Figure 7(b)). GRP profile shows zone of unclear radar reflection from 0 to 2 m because the survey line investigated on the earth-filled which separated rice fields, thus, in the upper zone was effected by the human activity. The zone of clayey sand deposit is paleo-channel underlain by reflection free zone. The boundary between top earth-filled layer and paleo-channel deposit layer displays in Figure 7(b) (CMN4). It consists of clayey sand and sandy clay. The apparent attenuation of radar signal increased as the content of clay-size particles in the subsurface increased [29]. This is explained by the organic and clay deposits, ground water level, roughly land surface and dense vegetation may attenuate a GPR signal concluded that fine-coarse interfaces cannot be detected using GPR method [15].

5 Conclusions

Trace of paleo-channels and meandered scar can be recognized based on surface geomorphological mapping from aerial photographs. Then, the characteristic of subsurface sedimentary deposition from GPR and ERT has been carried out together with sedimentological properties analysis from boreholes. The combination of resistivity ERT and sedimentological data in this study allowed us to precisely define ERT lithological classes and their relationship with sediment grain size and electrical resistivity values from subsurface (also see Table 1). In conclusion, we summarized the findings as follows.

- GPR profiles in this study show sedimentological structures as radar reflection facies. Sedimentological properties of subsurface from ERT and GPR provide a broad understanding of the subsurface geology. GPR proved valuable in depicting internal structure of fluvial sediments in particular point bar deposition (see in Figure 7). GPR radar facies from point bar deposit presents the inclined layer reflection of lateral accretion.
- ERT profiles of point bar and paleo-channel display low resistivity value associated with silty clay deposit from paleo-channel. Point bar deposit shows moderated to high resistivity from inversion model (100-1200 Ω·m) and it associated with loam and clayey to silty sand from location 1.
- ERT profile gathered from rice field (location 2) shows moderate to high resistivity value from buried paleo-channel. It is associated with clayey sand deposit. Channel geometry is approximately 30 m wide and 10 m depth. It is surrounded by low resistivity zone (0-36 Ω·m). This zone was interpreted as floodplain deposit that conforms to clayey silt and silty clay from borehole data. GPR survey on the western side of the ERT profile passes throughout clayey silt and silty clay layer, therefore, the radar signal shows parallel unclear reflection.
- Longitudinal ERT profile at Ban Wang Tabaek was investigated on floodplain and paleo-channels. High resistivity value (100-160 Ω·m) was interpreted as channel sediment deposit at 5 to 10 m depth. Borehole data are involved in loam and clayey to silty sand. Silty to sandy clay and clayey silt deposition conforms to low resistivity value (0-20 Ω·m), and it is applicable for floodplain deposit.

Moreover, the ERT lithological classes from this study can be applied for the ERT survey in adjacent area where are the same lithological conditions as alluvial sediment on sandstone bedrock. This study area mainly conprises floodplain and paleo-channels sediment succession, so the ERT is more effective for determining large scale subsurface fluvial landforms.

Acknowledgement: The 90th Anniversary of Chulalongkorn University Endowment provides fund to P.N.

M.C received funding from Ratchadapiseksomphot Foundation Endowment (WCU-58-18-CC). Authors would like to thank MESA Research Unit for laboratory facilities. Editor and two anonymous reviewers are thanked for the improvement of this manuscript.

References

[1] Nimnate, P.; Choowong, M.; Thitimakorn, T.; Hisada, K. Geomorphic criteria for distinguishing and locating abandoned channels from upstream part of mun river, khorat plateau, northeastern thailand. Environ Earth Sci 2017, 76.

[2] Alamry, A.S.; van der Meijde, M.; Noomen, M.; Addink, E.A.; van Benthem, R.; de Jong, S.M. Spatial and temporal monitoring of soil moisture using surface electrical resistivity tomography in mediterranean soils. CATENA 2017, 157, 388-396.

[3] Pellicer, X.M.; Gibson, P. Electrical resistivity and ground penetrating radar for the characterisation of the internal architecture of quaternary sediments in the midlands of ireland. Journal of Applied Geophysics 2011, 75, 638-647.

[4] Baines, D., Smith, D.G., Froese, D.G., Bauman, P., Nimeck, G. Electrical resistivity ground imaging (ergi): A new tool for mapping the lithology and geometry of channel-belts and valley-fills. Sedimentology 2002, 49, 441–449.

[5] Wisen, R., Auken, E., Dahlin, T. Combination of 1d laterally constrained inversion and 2d smooth inversion of resistivity data with a priori data from boreholes. Near Surface Geophysics 2005, 3, 71-79.

[6] Shaaban, F.F.; Shaaban, F.A. Use of two-dimensional electric resistivity and ground penetrating radar for archaeological prospecting at the ancient capital of egypt. Journal of African Earth Sciences 2001, 33, 661-671.

[7] Cassidy, N.J.; Calder, E.S.; Pavez, A.; Wooller, L. Studies in volcanology: the legacy of george walker. Thordarson, T.; Self, S.; Larsen, G.; Rowland, S.K.; Hoskuldsson, A., Eds. Geological Society of London: UK, 2009; Vol. 2, pp 181-210.

[8] Colombera, L.; Mountney, N.P.; McCaffrey, W.D. A quantitative approach to fluvial facies models: Methods and example results. Sedimentology 2013, 60, 1526–1558.

[9] Reesink, A.J.H.; Ashworth, P.J.; Sambrook Smith, G.H.; Best, J.L.; Parsons, D.R.; Amsler, M.L.; Hardy, R.J.; Lane, S.N.; Nicholas, A.P.; Orfeo, O., et al. Scales and causes of heterogeneity in bars in a large multi-channel river: Río paraná, argentina. Sedimentology 2014, 61, 1055-1085.

[10] Dheeradilok, P. Mineral resources and landuse planning for industrial development in nakhon ratchasrima, northeastern thailand. Journal of Southeast Asian Earth Sciences 1993, 8, 567-571.

[11] Storz, H.; Storz, W.; Jacobs, F. Electrical resistivity tomography to investigate geological structures of the earth's upper crust. Geophysical Prospecting 2000, 48, 455-471.

[12] Rey, J.; Martínez, J.; Hidalgo, M.C. Investigating fluvial features with electrical resistivity imaging and ground-penetrating radar: The guadalquivir river terrace (jaen, southern spain). Sedimentary Geology 2013, 295, 27-37.

[13] Okpoli, C.C. Sensitivity and resolution capacity of electrode configurations. International Journal of Geophysics 2013, 2013, 1-12.

[14] Jol, H.M.; Smith, D.G. Ground penetrating radar surveys of peatlands for oilfield pipelines in canada. Journal of Applied Geophysics 1995, 34, 109-123.

[15] Słowik, M. Reconstructing migration phases of meandering channels by means of ground-penetrating radar (gpr): The case of the obra river, poland. Journal of Soils and Sediments 2011, 11, 1262-1278.

[16] Davis, J.L.; Annan, A.P. Ground-penetrating radar for high-resolution mapping of soil and rock stratigraphy. Geophysical Prospecting 1989, 37, 531-551.

[17] Słowik, M. Influence of measurement conditions on depth range and resolution of gpr images: The example of lowland valley alluvial fill (the obra river, poland). Journal of Applied Geophysics 2012, 85, 1-14.

[18] Hickin, A.S.; Kerr, B.; Barchyn, T.E.; Paulen, R.C. Using ground-penetrating radar and capacitively coupled resistivity to investigate 3-d fluvial architecture and grain-size distribution of a gravel floodplain in northeast british columbia, canada. Journal of Sedimentary Research 2009, 79, 457-477.

[19] Bersezio, R.; Giudici, M.; Mele, M. Combining sedimentological and geophysical data for high-resolution 3-d mapping of fluvial architectural elements in the quaternary po plain (italy). Sedimentary Geology 2007, 202, 230-248.

[20] Singh, K.K.K. Application of ground penetrating radar for hydrogeological study. Journal of Scientific & Industrial Research 2006, 65, 160-164.

[21] Rey, J.; Martínez, J.; Hidalgo, M.C. Investigating fluvial features with electrical resistivity imaging and ground-penetrating radar: The guadalquivir river terrace (jaen, southern spain). Sedimentary Geology 2013, 295, 27-37.

[22] Bano, M.; Marquis, G.; Nivière, B.; Maurin, J.C.; Cushing, M. Investigating alluvial and tectonic features with ground-penetrating radar and analyzing diffractions patterns. Journal of Applied Geophysics 2000, 43, 33-41.

[23] Pueyo-Anchuela, Ó.; Casas-Sainz, A.M.; Pocoví Juan, A.; Soriano, M.A. Applying gpr-amplitude wave maps and am-scans as a semi-quantitative approach to the internal structure of sediments. Journal of Applied Geophysics 2011, 75, 151-160.

[24] Froese, D.G.; Smith, D.G.; Clement, D.T. Characterizing large river history with shallow geophysics: Middle yukon river, yukon territory and alaska. Geomorphology 2005, 67, 391-406.

[25] Martinez, A.; Byrnes, A.P. Modeling dielectric-constant values of geologic materials: An aid to ground-penetrating radar data collection and interpretation. Kansas Geological Survey: 2001; Vol. 247, p 32.

[26] Woodward, J.; Ashworth, P.J.; Best, J.L.; Smith, S.G.H.; Simpson, C.J. Ground penetrating radar in sediments. Bristow, C.S.; Jol, H.M., Eds. The Geological Society of London: London, 2003; Vol. 221, pp 127-142.

[27] Vandenberghe, J.; van Overmeeren, R.A. Ground penetrating radar images of selected fluvial deposits in the netherlands. Sedimentary Geology 1999, 128, 245-270.

[28] Brierley, G.J.; Hickin, E.J. Channel planform as a non-controlling factor in fluvial sedimentology: The case of the squamish river floodplain, british columbia. Sedimentary Geology 1991, 75, 67-83.

[29] Beres, M.J.; Haeni, F.P. Application of ground-penetrating- radar methods in hydrologic studies. Ground water 1991, 29, 375-386.

[30] Skellya, R.L.; Bristowb, C.S.; Ethridgea, F.G. Architecture of channel-belt deposits in an aggrading shallow sandbed braided river: The lower niobrara river, northeast nebraska. Sedimentary Geology 2003, 158, 249-270.

[31] Bowling, J.C.; Rodriguez, A.B.; Harry, D.L.; Zheng, C. Delineating alluvial aquifer heterogeneity using resistivity and gpr data. Ground water 2005, 43, 890-903.

[32] Folk, R.L. The distinction between grain size and mineral composition in sedimentary-rock nomenclature. The Journal of Geology 1954, 62, 344-359.

[33] Flemming, B.W. A revised textural classification of gravel-free muddy sediments on the basis of ternary diagrams. Continental Shelf Research 2000, 20, 1125-1137.

[34] Meesook, A.; Saengsrichan, W. Geology of thailand. 2nd Edition ed.; Ridd, M.F.; Barber, A.J.; Crow, M.J., Eds. Geological Society: North America, 2011; pp 151-184.

[35] Reynolds, S.; Johnson, J.; Michael, T.; Paul, K.; Carter, C. Exploring geology. 2 ed.; McGraw-Hill Science: 2012; Vol. 2016, p 648.